Vaccinia Virus-Induced Cell Motility Requires F11L-Mediated Inhibition of RhoA Signaling

Article *in* Science · February 2006

DOI: 10.1126/science.1122411 · Source: PubMed

5 authors, including:

Ferran Valderrama
City St George's, University of London
34 PUBLICATIONS **1,658** CITATIONS
SEE PROFILE

João V Cordeiro
Universidade NOVA de Lisboa
33 PUBLICATIONS **970** CITATIONS
SEE PROFILE

Friedrich Frischknecht
Heidelberg University
287 PUBLICATIONS **8,670** CITATIONS
SEE PROFILE

Michael Way
The Francis Crick Institute
312 PUBLICATIONS **14,368** CITATIONS
SEE PROFILE

previous studies that found natural sequence variation within this domain in soil bacteria (*19*). Knowledge of such natural variations could complement studies on clinical isolates to guide the rational development of next-generation fluoroquinolones that will be active against resistant strains.

Resistance to macrolide antibiotics in pathogens of clinical significance has increased considerably over recent decades and is commonly a result of antibiotic efflux and ribosomal protection mechanisms (*20*, *21*). Substantial levels of macrolide resistance were also detected in our soil isolate library, both to the natural product erythromycin (introduced in 1952, 27%), and the semisynthetic telithromycin (FDA-approved in 2004, 17%). The high frequency of telithromycin resistance was particularly intriguing, because telithromycin is known for its activity against macrolide-resistant bacteria.

Five percent of library isolates detoxified telithromycin in culture media (Table 1). One of these, *Streptomyces* strain Ja#7 (MIC of 32 μg/ml), completely modified telithromycin to an inactive hydrophilic product with a mass of 973.6 daltons (Fig. 3). This addition of 162 daltons to telithromycin (811.7 daltons) is a signature indicator of monoglycosylation. Large-scale purification of the product, followed by multidimensional and multinuclear magnetic resonance analysis, confirmed that the inactive product was 2′-*O*-glucosyl-telithromycin (table S1).

Modification of the cladinose 2′-OH of erythromycin is known to result in antibiotic resistance (*22*, *23*). However, Ja#7, despite its ability to inactivate telithromycin, was unable to completely inactivate erythromycin or its derivative clarithromycin under identical conditions. Thus, a distinct mechanism seems to be operating. Given the abundance of resistance determinants in streptomycetes that are homologous to those in clinically significant pathogens (*5*, *24*, *25*), it is evident that once this mechanism is fully characterized, it should be monitored as telithromycin use increases clinically and resistant organisms inevitably emerge.

This study provides an analysis of the antibiotic resistance potential of soil microorganisms. The frequency of high-level resistance seen in the study to antibiotics that have for decades served as gold-standard treatments, as well as those only recently approved for human use, is remarkable. No class of antibiotic was spared with respect to bacterial target or natural or synthetic origin. Although this study does not provide evidence for the direct transfer of resistance elements from the soil resistome to pathogenic bacteria, it identifies a previously underappreciated density and concentration of environmental antibiotic resistance. The level and diversity of resistance uncovered in this work is only partially reflective of the true extent of the environmental resistome, because this study was restricted exclusively to culturable spore-forming bacteria, which represent only a fraction of soil-dwelling bacteria. For example, a recent soil metagenome analysis uncovered several aminoglycoside resistance genes in uncultured organisms (*26*). Furthermore, the primary screen was conducted at high antibiotic concentrations, thereby excluding phenotypes exhibiting low to intermediate resistance. The level of resistance genes in the environment is therefore very likely to be substantially higher and the antibiotic resistome much more extensive than this study reveals.

The survey of antibiotic resistance mechanisms can assist the elucidation of novel mechanisms that may emerge clinically, as well as serve as a foundation for new antibiotic development. In addition, the study of enzymatic inactivation could lead to the development of inhibitors for combination therapies to restore antimicrobial activity.

References and Notes

1. T. Kieser, M. J. Bibb, M. J. Buttner, K. F. Chater, D. A. Hopwood, *Practical Streptomyces Genetics* (John Innes Foundation, Norwich, UK, ed. 1, 2000).
2. B. K. Hubbard, C. T. Walsh, *Angew. Chem. Int. Ed. Engl.* **42**, 730 (2003).
3. E. Cundliffe *et al.*, *Antonie Leeuwenhoek* **79**, 229 (2001).
4. J. Davies, *Science* **264**, 375 (1994).
5. C. G. Marshall, I. A. Lessard, I. Park, G. D. Wright, *Antimicrob. Agents Chemother.* **42**, 2215 (1998).
6. H. J. Hong, M. S. Paget, M. J. Buttner, *Mol. Microbiol.* **44**, 1199 (2002).
7. L. Guardabassi, A. Dalsgaard, *Appl. Environ. Microbiol.* **70**, 984 (2004).
8. C. T. Walsh, *Antibiotics: Actions, Origins, Resistance* (American Society for Microbiology Press, Washington, DC, ed. 1, 2003).
9. H. Myllykallio, D. Leduc, J. Filee, U. Liebl, *Trends Microbiol.* **11**, 220 (2003).
10. D. R. Snydman, N. V. Jacobus, L. A. McDermott, J. R. Lonks, J. M. Boyce, *Antimicrob. Agents Chemother.* **44**, 3447 (2000).
11. I. A. Critchley *et al.*, *Antimicrob. Agents Chemother.* **47**, 1689 (2003).
12. W. E. Alborn Jr., N. E. Allen, D. A. Preston, *Antimicrob. Agents Chemother.* **35**, 2282 (1991).
13. D. Jung, A. Rozek, M. Okon, R. E. Hancock, *Chem. Biol.* **11**, 949 (2004).
14. M. Debono *et al.*, *J. Antibiot. (Tokyo)* **41**, 1093 (1988).
15. M. Gellert, K. Mizuuchi, M. H. O'Dea, T. Itoh, J. I. Tomizawa, *Proc. Natl. Acad. Sci. U.S.A.* **74**, 4772 (1977).
16. H. Peng, K. J. Marians, *J. Biol. Chem.* **268**, 24481 (1993).
17. L. J. Piddock, *Drugs* **58** (suppl. 2), 11 (1999).
18. J. H. Tran, G. A. Jacoby, *Proc. Natl. Acad. Sci. U.S.A.* **99**, 5638 (2002).
19. B. Waters, J. Davies, *Antimicrob. Agents Chemother.* **41**, 2766 (1997).
20. G. V. Doern *et al.*, *Antimicrob. Agents Chemother.* **45**, 1721 (2001).
21. P. Descheemaeker *et al.*, *J. Antimicrob. Chemother.* **45**, 167 (2000).
22. N. Noguchi *et al.*, *Antimicrob. Agents Chemother.* **39**, 2359 (1995).
23. E. Cundliffe, *Antimicrob. Agents Chemother.* **36**, 348 (1992).
24. C. J. Thompson, G. S. Gray, *Proc. Natl. Acad. Sci. U.S.A.* **80**, 5190 (1983).
25. I. Chopra, M. Roberts, *Microbiol. Mol. Biol. Rev.* **65**, 232 (2001).
26. C. S. Riesenfeld, R. M. Goodman, J. Handelsman, *Environ. Microbiol.* **6**, 981 (2004).

27. We thank K. P. Koteva for helpful discussions and analytical expertise; B. Ghadaki, C. Capone, and T. Patel for help with construction of the soil library; and S. Projan, P. Bradford, and J. Silverman for careful reading of the manuscript. This work was funded by the Canadian Institutes of Health Research and by a Canada Research Chair to G.D.W. Accession numbers for nucleotide sequences deposited in GenBank run consecutively from DQ311010 to DQ311051.

Supporting Online Material

www.sciencemag.org/cgi/content/full/311/5759/374/DC1
Materials and Methods
Figs. S1 to S4
Tables S1 to S5
References

30 September 2005; accepted 12 December 2005
10.1126/science.1120800

Vaccinia Virus–Induced Cell Motility Requires F11L-Mediated Inhibition of RhoA Signaling

Ferran Valderrama, João V. Cordeiro, Sibylle Schleich, Friedrich Frischknecht,* Michael Way†

RhoA signaling plays a critical role in many cellular processes, including cell migration. Here we show that the vaccinia F11L protein interacts directly with RhoA, inhibiting its signaling by blocking the interaction with its downstream effectors Rho-associated kinase (ROCK) and mDia. RNA interference–mediated depletion of F11L during infection resulted in an absence of vaccinia-induced cell motility and inhibition of viral morphogenesis. Disruption of the RhoA binding site in F11L, which resembles that of ROCK, led to an identical phenotype. Thus, inhibition of RhoA signaling is required for both vaccinia morphogenesis and virus-induced cell motility.

The spatial and temporal regulation of cell adhesion and motility is essential during development and throughout the lifetime of multicellular organisms (*1*, *2*). Deregulation of these two fundamental cellular processes frequently occurs during pathological situations such as tumor cell metastasis (*3*, *4*). Dramatic changes in cell migration and adhesion, as well as loss of contact inhibition, are also observed during many viral infections, including that of vaccinia virus (*5*, *6*). In contrast to the wild-type Western-Reserve (WR) virus,

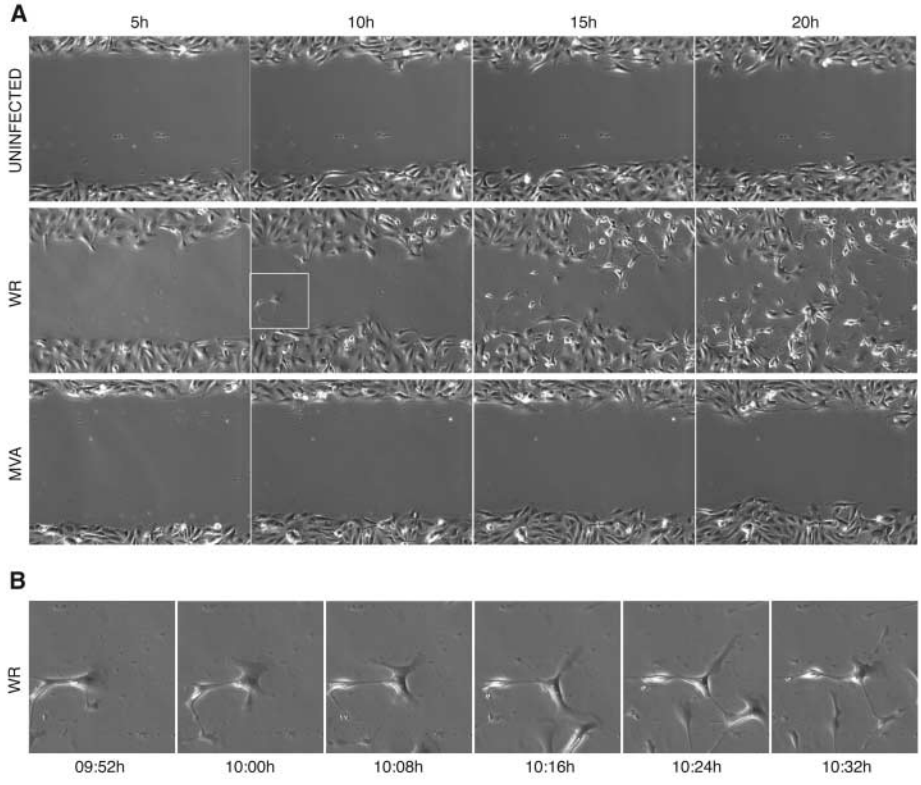

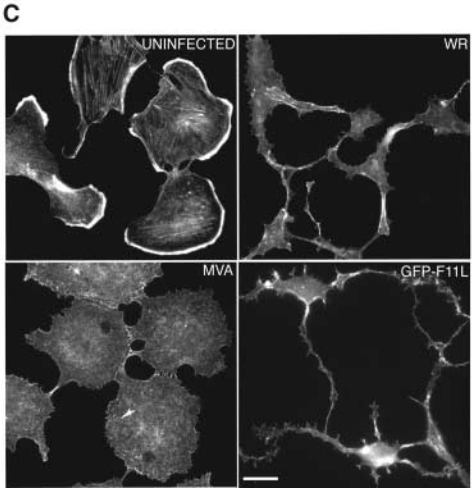

Fig. 1. F11L is required for vaccinia-induced cell motility. (**A**) Phase contrast movie stills from wound-healing assays reveal that BS-C-1 cells do not migrate into the wound site in the absence of serum (top). In contrast, infection with the wild-type Western Reserve virus (WR, middle), but not modified vaccinia Ankara virus (MVA, bottom), induces BS-C-1 cell migration. The time after the initial wound (hours) is indicated. (**B**) Enlargement of the WR-infected cell highlighted in (A) (box, 10h) reveals that migrating cells fail to retract their trailing edge and extend multiple lamellipodia. (**C**) Immunofluorescence analysis reveals that WR and MVA infection results in a loss of actin stress fibers but that only WR induces the projection phenotype. Expression of GFP-F11L induced the projection phenotype in MVA-infected cells. Bar, 10 μm.

we found that modified vaccinia Ankara (MVA), a highly attenuated virus strain containing multiple mutations and deletions in its genome (*7*–*9*), did not induce cell migration or cellular projections in the absence of serum (Fig. 1, Movies S1 to S3) (*10*).

To determine the gene (or genes) absent in MVA that are responsible for vaccinia-induced cell motility, we examined the ability of a series of recombinant MVA virus strains, which contained portions of DNA from its parental strain (*9*), to induce the projection phenotype. Only MVA recombinants rescued with cosmid 44 induced a projection phenotype (fig. S1), suggesting that the genomic region covered by cosmid 44 contained a gene (or genes) required for vaccinia-induced cell motility. Of the five genes disrupted or deleted in this genomic region, only one, F11L, or its green fluorescent protein (GFP)–tagged variant promoted the projection phenotype when expressed in MVA-infected cells (Fig. 1C, fig. S2) (*10*).

When expressed in uninfected cells, GFP-F11L induced a loss of actin stress fibers reminiscent of the dominant-negative RhoA-N19 (Fig. 2A). Furthermore, F11L inhibited stress fiber induction by coexpressed constitutively active Rho-V14 (Fig. 2A), suggesting that F11L might inhibit signaling by RhoA. To examine whether F11L interacted with RhoA or acted downstream of the guanosine triphosphatase (GTPase), we performed pull-down assays from cells coexpressing GFP-tagged RhoGTPases and F11L tagged with glutathione-*S*-transferase (GST) (*10*). RhoA but not Cdc42 or Rac copurified with F11L from cell extracts (Fig. 2B). Moreover, F11L interacted with both constitutively active RhoA-V14 and dominant-negative RhoA-N19 (Fig. 2B). Endogenous F11L and RhoA were also complexed with each other in vivo in infected cells (Fig. 2C). Moreover, a direct interaction between F11L and RhoA could be demonstrated with GST and His-tagged proteins produced in *Escherichia coli*.

Secondary-structure predictions suggest that F11L adopts a globular structure with an N-terminal domain (residues 1 to 222) rich in β sheet and a C-terminal helical domain (residues 223 to 345) containing at least one contiguous predicted helix longer than 50 residues. We found that the C-terminal helical domain of F11L but not the N-terminal region was able to interact directly with RhoA (fig. S3). Closer examination of the C-terminal region of F11L revealed that residues 299 to 312 share a limited homology to residues 998 to 1010 of Rho-associated kinase (ROCK) (fig. S3). This region of ROCK is known to mediate its interaction with RhoA (*11*). Substitution of four of the five identical residues with alanine substantially weakened the interaction between F11L and RhoA (Fig. 2D) (*10*). Combinations of double mutations resulted in a complete lack of binding (Fig. 2D). Thus, F11L appears to interact with RhoA in a manner similar to that of ROCK. Consistent with this hypothesis, the RhoA-V14E40L mutant that is deficient in ROCK binding (*12*) could not interact with F11L (Fig. 2E). In contrast to the wild-type protein, GFP-tagged F11L mutants deficient in Rho binding were also unable to stimulate the projection phenotype when expressed in MVA-infected cells (fig. S4). Thus, F11L inhibits the ability of the GTPase to signal during infection by binding directly to RhoA.

The failure of the rear of infected cells to detach and the formation of multiple lamellipodia at the front are very reminiscent of the effects of inhibition of ROCK in a variety of migrating cells (*13*–*16*). We examined whether the interaction of F11L with RhoA-V14 affected the ability of the GTPase to bind ROCK. F11L inhibited the ability of RhoA-V14 to

Cell Motility Laboratory, Cancer Research UK, London Research Institute, Lincoln's Inn Fields Laboratories, 44 Lincoln's Inn Fields, WC2A 3PX London, UK.

*Present address: Department of Parasitology, Heidelberg University School of Medicine, Im Neuenheimer Feld 324, 69120 Heidelberg, Germany.

†To whom correspondence should be addressed. E-mail: michael.way@cancer.org.uk

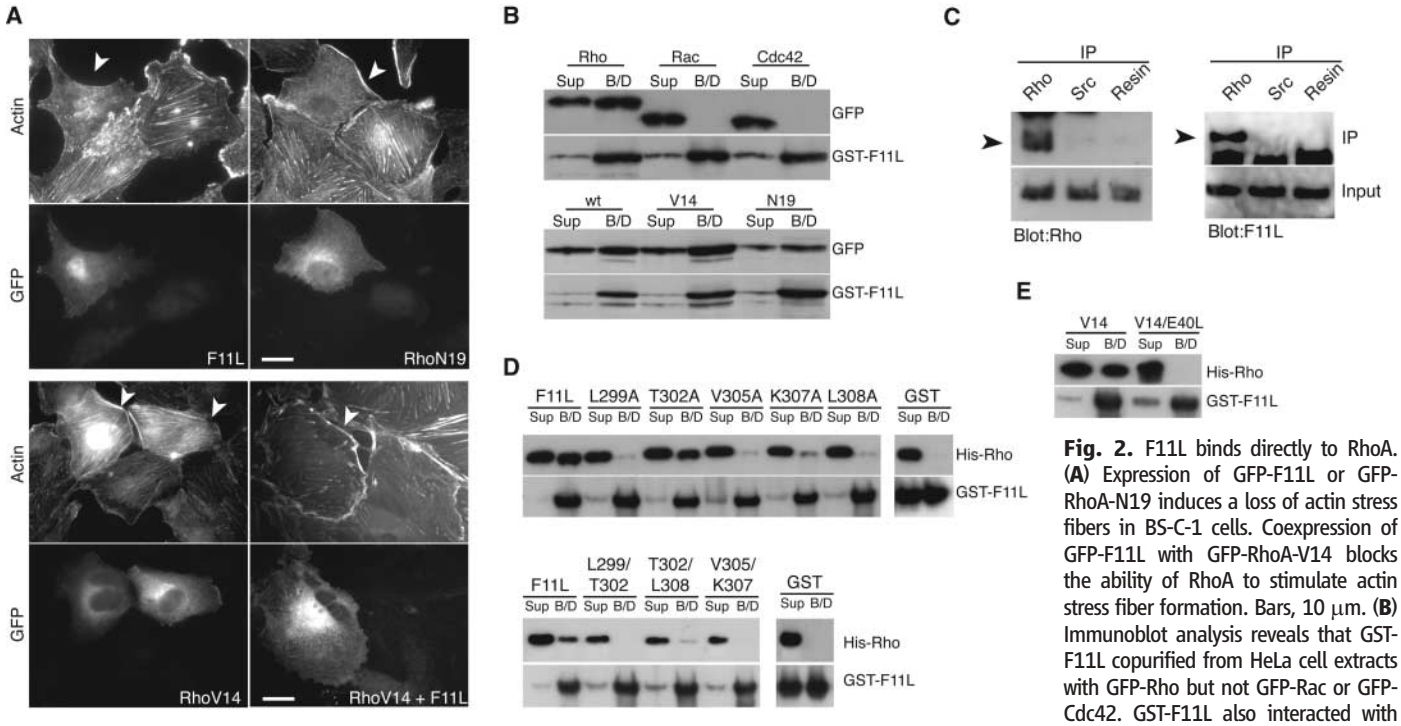

Fig. 2. F11L binds directly to RhoA. (**A**) Expression of GFP-F11L or GFP-RhoA-N19 induces a loss of actin stress fibers in BS-C-1 cells. Coexpression of GFP-F11L with GFP-RhoA-V14 blocks the ability of RhoA to stimulate actin stress fiber formation. Bars, 10 μm. (**B**) Immunoblot analysis reveals that GST-F11L copurified from HeLa cell extracts with GFP-Rho but not GFP-Rac or GFP-Cdc42. GST-F11L also interacted with GFP-RhoA-V14 and GFP-RhoA-N19. The supernatant (Sup) and bound (B/D) samples, together with the respective RhoGTPase or RhoA mutant, are indicated. (**C**) Immunoblot analysis of coimmunoprecipitation experiments revealed that F11L is complexed with RhoA in infected cells. (**D**) (Top) Immunoblot analysis of in vitro pull-down assays reveals that alanine substitution of conserved residues shared between F11L and ROCK substantially reduced the binding of F11L to RhoA. (Bottom) Double alanine substitutions in F11L resulted in a complete loss of binding. (**E**) Immunoblot analysis of in vitro pull-down assays reveals that F11L does not interact with Rho-V14/E40L.

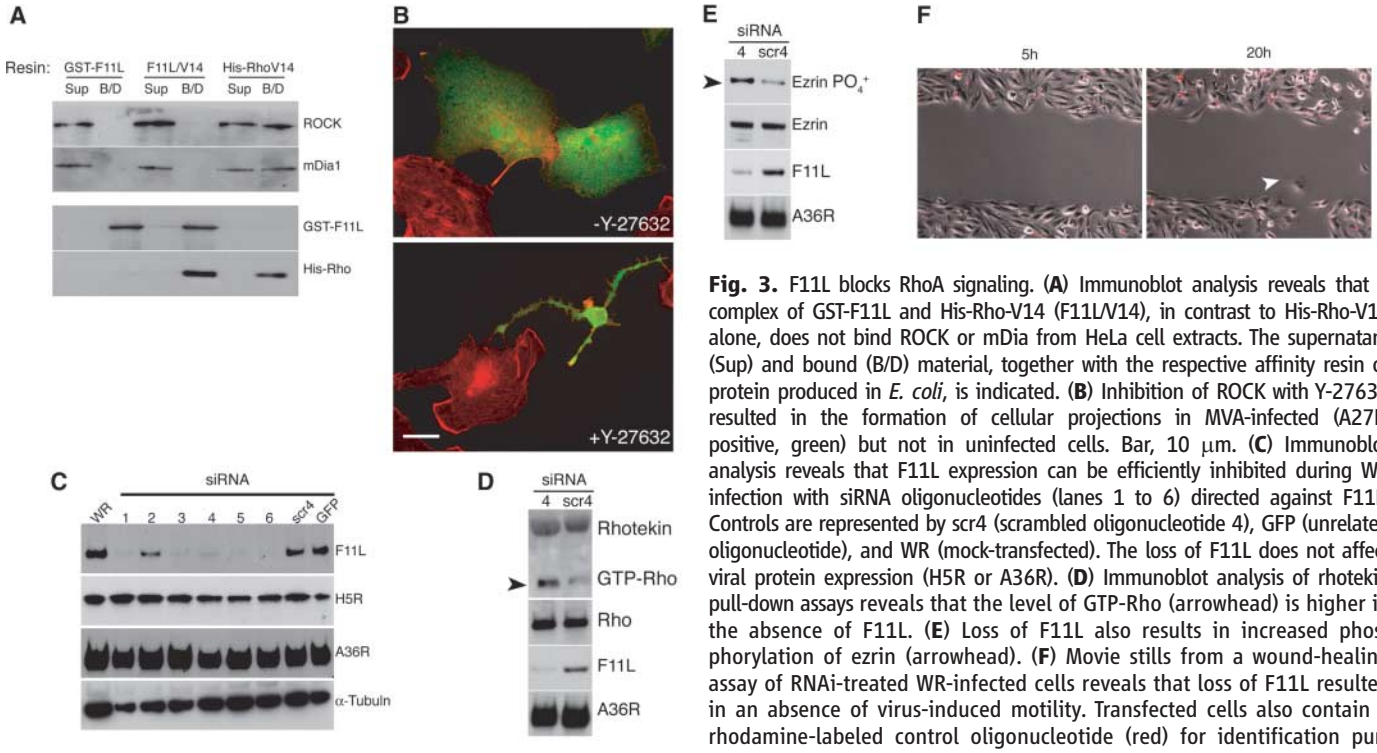

Fig. 3. F11L blocks RhoA signaling. (**A**) Immunoblot analysis reveals that a complex of GST-F11L and His-Rho-V14 (F11L/V14), in contrast to His-Rho-V14 alone, does not bind ROCK or mDia from HeLa cell extracts. The supernatant (Sup) and bound (B/D) material, together with the respective affinity resin of protein produced in *E. coli*, is indicated. (**B**) Inhibition of ROCK with Y-27632 resulted in the formation of cellular projections in MVA-infected (A27L-positive, green) but not in uninfected cells. Bar, 10 μm. (**C**) Immunoblot analysis reveals that F11L expression can be efficiently inhibited during WR infection with siRNA oligonucleotides (lanes 1 to 6) directed against F11L. Controls are represented by scr4 (scrambled oligonucleotide 4), GFP (unrelated oligonucleotide), and WR (mock-transfected). The loss of F11L does not affect viral protein expression (H5R or A36R). (**D**) Immunoblot analysis of rhotekin pull-down assays reveals that the level of GTP-Rho (arrowhead) is higher in the absence of F11L. (**E**) Loss of F11L also results in increased phosphorylation of ezrin (arrowhead). (**F**) Movie stills from a wound-healing assay of RNAi-treated WR-infected cells reveals that loss of F11L resulted in an absence of virus-induced motility. Transfected cells also contain a rhodamine-labeled control oligonucleotide (red) for identification purposes. The arrowhead indicates a single nontransfected cell, migrating into the wound. The time after the initial wound (hours) is indicated.

retain ROCK from HeLa cell extracts (Fig. 3A) (*10*). Treatment of MVA-infected cells with the ROCK inhibitor Y-27632 (*16*), although inducing the projection phenotype, was unable to stimulate cell migration (Fig. 3B), suggesting that modulation of additional signaling pathways are also required for vaccinia-induced cell motility. Consistent with this notion, F11L also inhibited the ability of RhoA to interact with

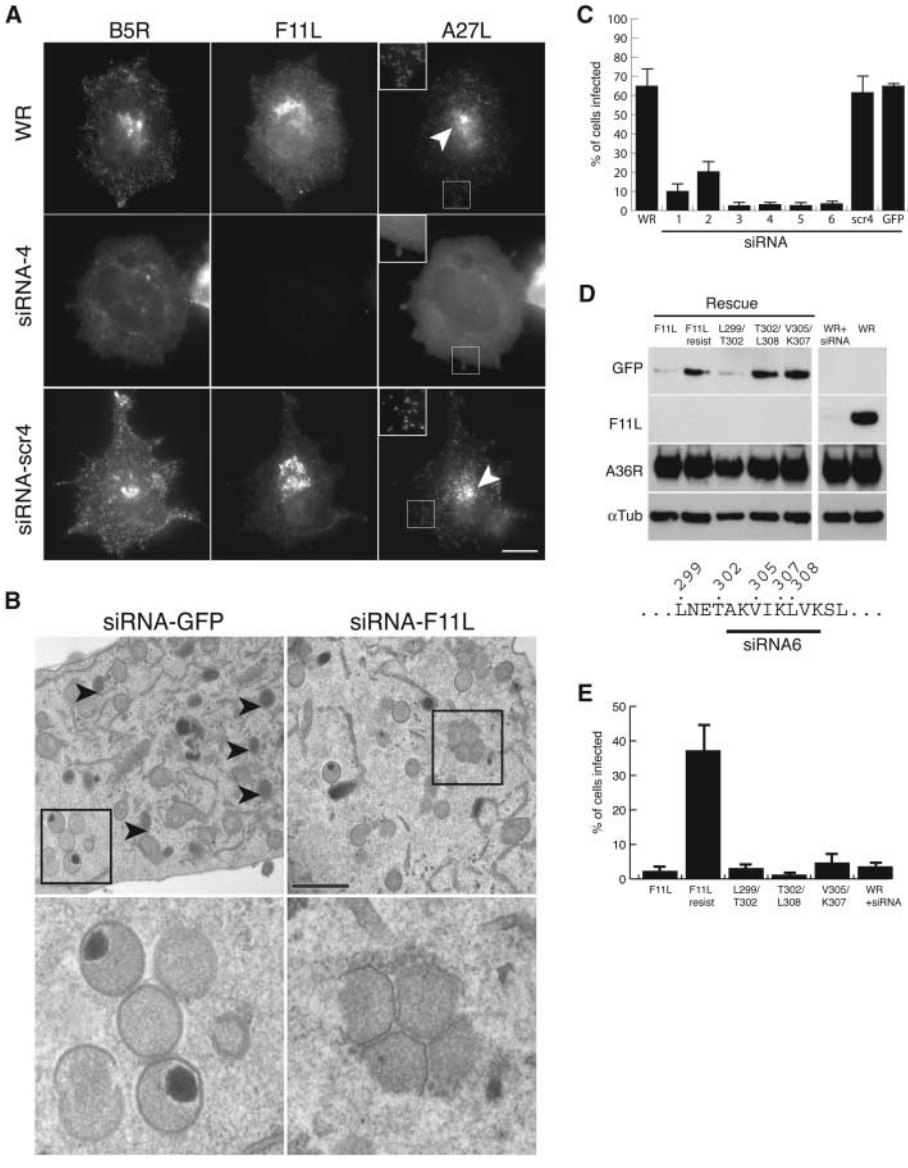

Fig. 4. Virus morphogenesis requires inhibition of RhoA signaling. (**A**) The absence of F11L resulted in disruption of perinuclear sites of virus assembly (arrowheads in WR and siRNA-scr4) and loss of assembled virus particles as judged by diffuse cytoplasmic localization of A27L and B5R (highlighted in the insets). Bar, 10 μm. (**B**) (Top) Epon sections of siRNA-treated HeLa cells infected with WR 8 hours after infection revealed that an absence of F11L resulted in loss of assembled intracellular mature virus particles (arrowheads). Immature virions were present in both samples, although their characteristic smooth curved profiles were often distorted (boxed areas are enlarged, bottom) in the absence of F11L. Bar, 1 μm. (**C**) Reinfection assays demonstrated that a loss of F11L expression resulted in a large reduction in the number of infectious particles released into the medium from WR-infected cells. Error bars represent the standard deviation of the mean from three independent experiments. (**D**) Immunoblot analysis of siRNA6-treated WR-infected cells expressing the indicated F11L rescue clone. Expression of the wild-type or L299/T302 mutant is inhibited by the siRNA6 oligonucleotide. In contrast, F11L resist, T302/L308, and V305/K307 are expressed because they contain point mutants that make them resistant to silencing by siRNA6 oligonucleotide. (**E**) Reinfection assays demonstrated that infectious virus particles are produced in siRNA6-treated WR-infected HeLa cells expressing F11L resist. In contrast, T302/L308 and V305/K307 mutants, which cannot bind RhoA, do not rescue virus morphogenesis in the absence of endogenous F11L expression. Error bars represent the standard deviation of the mean from three independent experiments.

mDia (Fig. 3A). To analyze whether F11L does indeed modulate RhoA signaling, we examined the level of GTP-bound RhoA in WR-infected cells in the absence of F11L. Transfection of small interfering RNA (siRNA) oligonucleotides against F11L before vaccinia infection markedly suppressed expression of the protein without affecting the levels of other viral proteins (Fig. 3C) (*10*). A reduction in the level of F11L expression resulted in an increase of GTP-bound RhoA in infected cell extracts (Fig. 3D). Concomitantly, the phosphorylation level of the Rho effector ezrin was increased and virus-induced cell motility was lost (Fig. 3, E and F; Movie S4). Thus, F11L inhibits the ability of RhoA to signal to its downstream effectors during vaccinia virus infection.

The sequence of F11L is strongly conserved within the genome of orthopoxviruses, suggesting that the protein may play an important role in the vaccinia virus life cycle. Indeed F11L, which is expressed from as early as 2 hours after infection, is associated with perinuclear viral factories (fig. S5). To elucidate the function of F11L in the vaccinia life cycle, we set out to delete the F11L gene in the WR genome by homologous recombination. However, in agreement with Kato *et al*. (*17*), we were unable to isolate recombinants lacking the F11L gene when using this strategy, suggesting that it is essential for the production of infectious virus in culture. To explore this possibility, we analyzed the effects of siRNA-mediated ablation of F11L expression on the vaccinia life cycle. Loss of F11L expression resulted in an absence of assembled virus particles as judged by the diffuse cytoplasmic localization of mature virus particle markers such as A27L and B5R (Fig. 4A). Analysis of siRNA-treated cells by electron microscopy (*10*) confirmed that the absence of F11L resulted in a defect in morphogenesis, with a substantial loss of assembled mature virus particles and an accumulation of aberrant immature virions (IVs) (Fig. 4B). An accumulation of IVs is also observed during the abortive life cycle of MVA in HeLa cells (*18*, *19*).

To examine whether the loss of F11L expression reduced production of infectious virus particles, we performed reinfection experiments using the tissue culture medium from siRNA-transfected cells (*10*). We observed up to a ~14-fold reduction in the number of infectious virus particles released into the tissue culture medium when compared with untreated cells (Fig. 4C). To analyze if the interaction of F11L with RhoA is required for viral morphogenesis, we examined whether expression of RNAi-resistant F11L mutants deficient in RhoA binding would rescue production of infectious virus in siRNA-transfected cells. In contrast to the wild-type protein, expression of F11L mutants deficient in RhoA binding were unable to rescue production of in-

fectious virus in siRNA-transfected cells (Fig. 4, D and E). Thus, F11L-mediated inhibition of RhoA signaling is required for both vaccinia morphogenesis and infection-induced cell motility. Our observations may also explain, at least in part, why MVA, which lacks functional F11L, is unable to replicate in most cell types in culture (*7*–*9*). They also offer molecular insights into the mechanism by which vaccinia induces cell migration (*5*, *6*). One can envisage that migration of an infected cell will increase the efficiency of virus spread because extracellular virus particles associated with the plasma membrane, which are responsible for direct cell to cell spread, will come into contact with more neighboring noninfected cells than they would if the infected cell were static.

References and Notes

1. A. J. Ridley *et al.*, *Science* **302**, 1704 (2003).
2. P. Martin, S. M. Parkhurst, *Development* **131**, 3021 (2004).
3. P. Friedl, K. Wolf, *Nat. Rev. Cancer* **3**, 362 (2003).
4. N. O. Carragher, M. C. Frame, *Trends Cell Biol.* **14**, 241 (2004).
5. C. M. Sanderson, G. L. Smith, *J. Virol.* **72**, 9924 (1998).
6. C. M. Sanderson, M. Way, G. L. Smith, *J. Virol.* **72**, 1235 (1998).
7. M. W. Carroll, B. Moss, *Virology* **238**, 198 (1997).
8. I. Drexler, K. Heller, B. Wahren, V. Erfle, G. Sutter, *J. Gen. Virol.* **79**, 347 (1998).
9. L. S. Wyatt *et al.*, *Virology* **251**, 334 (1998).
10. See supporting data on *Science* Online.
11. R. Dvorsky, L. Blumenstein, I. R. Vetter, M. R. Ahmadian, *J. Biol. Chem.* **279**, 7098 (2004).
12. E. Sahai, A. S. Alberts, R. Treisman, *EMBO J.* **17**, 1350 (1998).
13. R. A. Worthylake, S. Lemoine, J. M. Watson, K. Burridge, *J. Cell Biol.* **154**, 147 (2001).
14. R. A. Worthylake, K. Burridge, *J. Biol. Chem.* **278**, 13578 (2003).
15. A. Smith, M. Bracke, B. Leitinger, J. C. Porter, N. Hogg, *J. Cell Sci.* **116**, 3123 (2003).
16. K. Riento, A. J. Ridley, *Nat. Rev. Mol. Cell Biol.* **4**, 446 (2003).
17. S. E. Kato, F. A. Greco, C. R. Damaso, R. C. Condit, N. Moussatche, *J. Virol. Methods* **115**, 31 (2004).
18. M. C. Sancho, S. Schleich, G. Griffiths, J. Krijnse-Locker, *J. Virol.* **76**, 8318 (2002).
19. J. C. Gallego-Gomez *et al.*, *J. Virol.* **77**, 10606 (2003).

20. We thank J. Krijnse-Locker (European Molecular Biology Laboratory, Heidelberg, Germany) and A. Alberts (Van Andel Research Institute, Grand Rapids, MI) for providing antibodies. We also thank B. Moss (National Institute of Allergy and Infectious Diseases, Bethesda, MD) for providing MVA recombinants, E. Sahai (Cancer Research UK, London) for the RhoV14E40L clone, and P. Traktman (Department of Microbiology and Molecular Genetics, WI) for discussions about siRNA in infected cells. We thank the Way lab, E. Sahai, N. Hogg, and R. Treisman (Cancer Research UK, London) for helpful comments on the manuscript. F.V. was supported by a European Community Marie Curie Fellowship (Number HPMF-CT-2000-01021).

Supporting Online Material

www.sciencemag.org/cgi/content/full/311/5759/377/DC1
Materials and Methods
Figs. S1 to S6
Movies S1 to S4
References

9 November 2005; accepted 20 December 2005
10.1126/science.1122411

Core Knowledge of Geometry in an Amazonian Indigene Group

Stanislas Dehaene,[1,2]* Véronique Izard,[1] Pierre Pica,[3] Elizabeth Spelke[4]

Does geometry constitute a core set of intuitions present in all humans, regardless of their language or schooling? We used two nonverbal tests to probe the conceptual primitives of geometry in the Mundurukú, an isolated Amazonian indigene group. Mundurukú children and adults spontaneously made use of basic geometric concepts such as points, lines, parallelism, or right angles to detect intruders in simple pictures, and they used distance, angle, and sense relationships in geometrical maps to locate hidden objects. Our results provide evidence for geometrical intuitions in the absence of schooling, experience with graphic symbols or maps, or a rich language of geometrical terms.

> *Through natural selection, our mind has adapted to the conditions of the external world,* […] *it has adopted the geometry most advantageous to our species; or, in other words, the most convenient.*
> –Henri Poincaré, *La Science et l'Hypothèse*

Euclidean geometry is one of the deepest and oldest products of human reason, but its foundations remain elusive. Many of its propositions—that two points determine a line, or that three orthogonal axes localize a point—are judged to be self-evident (*1*, *2*) and yet have been questioned on the basis of logical argument, physical theory, or experiment [(*3*–*5*); for a historical review, see (*6*)]. Here we ask whether the conceptual principles of geometry are inherent in the human mind, by studying the spontaneous geometrical knowledge of the Mundurukú, an Amazonian indigene group (*7*). The present data were collected by one of us (P.P.) during a field trip in 2004–2005 to remote sites along the Cururu river. Most of the children and adults who took part in our experiments inhabit scattered, isolated villages and have little or no schooling, rulers, compasses, or maps. Furthermore, the Mundurukú language has few words dedicated to arithmetical, geometrical, or spatial concepts, although a variety of metaphors are spontaneously used (see Supporting Online Material for a list).

Our first test [inspired from (*8*)] was designed to probe the Mundurukú's intuitive comprehension of the basic concepts of geometry, including points, lines, parallelism, figures, congruence, and symmetry (*9*). For each such concept, we designed an array of six images, five of which instantiated the desired concept while the remaining one violated it (Fig. 1). The participants were asked, in their language, to point to the "weird" or "ugly" one. Care was taken to minimize cues other than the desired conceptual relation that could be used to identify the target. For instance, if the desired concept was "trapezoid," the target was a nontrapezoidal quadrilateral whose size and orientation fell within the range of variation of the other five trapezoids. There are many ways in which the participants could have selected an odd picture out of the six, including size, orientation, or personal preference. If the Mundurukú share with us the conceptual primitives of geometry, however, they should infer the intended geometrical concept behind each array and therefore select the discrepant image.

All participants, even those aged 6, performed well above the chance level of 16.6% (average 66.8% correct, minimum 44.2% correct, $P < 0.001$). Performance was higher than chance in all but 6 of the 45 slides ($P \ll 0.001$) and was indistinguishable for Mundurukú adults and children. There was no significant influence of the bilingualism or schooling exhibited by some of the participants (*9*). As shown in Fig. 1, the Mundurukú succeeded remarkably well with the core concepts of topology (e.g., connectedness), Euclidan geometry (e.g., line, point, parallelism, and right angle), and basic geometrical figures (e.g., square, triangle, and circle). They experienced more difficulty, but still achieved higher-than-chance performance, in detecting symmetries and metric properties (e.g., equidistance of points). They performed poorly only in two domains: a series of slides assessing geometrical transformations, for instance, by depicting two triangles in a mirror-symmetry relation; and another two slides in which the intruder shape was a randomly oriented mirror image of the other shapes. Interestingly, both types of slides require a mental transformation of one shape into another, followed by a second-order judgment about the nature of this transformation. It is possible that geometrical transformations are inherently more difficult mathematical

[1]INSERM-CEA Cognitive Neuroimaging Unit, Service Hospitalier Frédéric Joliot, Commissariat à l'Energie Atomique, 91401 Orsay Cedex, France. [2]Collège de France, 11, place Marcelin Berthelot, 75231 Paris Cedex 05, France. [3]Unité Mixte de Recherche 7023 "Formal Structure of Language," CNRS and Paris VIII University, Paris, France. [4]Psychology Department, Harvard University, Cambridge, MA 02139, USA.

*To whom correspondence should be addressed. E-mail: dehaene@shfj.cea.fr